Estimation of the road traffic sound levels in urban areas based on non-negative matrix factorization techniques

Jean-Rémy GLOAGUEN
Arnaud Can
LAE
Ifsttar
jean-remy.gloaguen@ifsttar.fr

Mathieu Lagrange
Jean-François Petiot
LS2N, CNRS
École Centrale de Nantes

Abstract

The advent of low cost acoustic monitoring devices raises new interesting approaches for improving the monitoring of the acoustic quality of urban areas. State of the art approaches target road traffic noise maps and consider, as input, an estimate of the number and the speed of vehicles in major traffic lanes. Follows a prediction procedure that outputs an acoustic pressure level at any location in the modeled area.

Considering as input the acoustic pressure measured in many locations using a sensor grid approach would greatly complement and improve the quality of the predicted pressure values. Among the technical issues that raise this kind of innovative approaches, there is a need to identify which part of the overall acoustic pressure level is due to the road traffic.

In this paper, several techniques based on non-negative factorization framework are studied in this application scenario on a simulated sound scene corpus. The task being to the best of our knowledge never been considered in the literature, we propose an experimental protocol to validate the studied approaches that complies with standard reproducible research recommendations. The results show the interest of our proposed approach for such sound environments as it improves the estimation of the road traffic sound level compared to basic methods.

1 Introduction

With the introduction of the European Directive 2002/EC/49, cities over 100 000 inhabitants have to produce road traffic noise maps. These maps depict the sound level distribution over the city and an estimation of the number of city dwellers exposed to high noise levels. These maps play both an important communication role and help drawing up action plans to reduce noise exposure. Road traffic noise maps are the result of a simulation process based on the estimation of the traffic density on the main roads and the use of sound propagation modelling. They express as output L_{DEN} and L_N values, which are *Day-Evening-Night* and *Night* equivalent A-weighted sound levels respectively. Altough very useful, the produced noise maps introduce lot of uncertainty generated by the numerical tools [1] or by the different calculation methodologies used [2][3], despite the long data collection and calculation times. In addition, the usual road traffic noise maps are static, aggregating the exposure into indicators L_{DEN} and L_N, that ignore the sound levels evolution throughout the day. The use of acoustic measurements could facilitate their updating or even the generation of dynamic maps [4]. These measurements can be performed at fixed stations spread all over the cities [5] [6], which would make available of the long-term evolution of the traffic noise levels. It can also be performed with mobile stations [7] [8] covering a larger area with fewer sensors but also sparse time periods.

Currently, sensor networks in cities are spread for multiple applications (air quality assessment, measurement of meteorological parameters ...), including the assessment of urban noise levels. The DYNAMAP project [9] studied the deployment and feasibility of such installations focusing on sensor installations on specific roads at the city scale in Milan and Rome [10]. The SONYC project (Sounds Of New-York City) aims to deploy a sensor network in New-York City for the purpose of monitoring constantly the noise pollution in the city [11]. In order to better know the urban sound environment, sensors are coupled with a detection tool that identifies the sound sources present [12]. In a similar way, but reduced to few neighborhoods with a denser network, the CENSE project[1] [13] aims to combine *in situ* observations, from a sensor network, and numerical data, from noise modeling, through data assimilation techniques.

Prior to data assimiliation, the issue of the correct

[1] http://cense.ifsttar.fr/

estimation of the traffic sound level from acoustic measurements is still unsolved [5]. Mainly because the urban sound environment is a complex environment gathering lots of different sounds (car passages, voices, whistling bird, car horn, airplanes...) that overlap. Consequently, the traffic sound level estimation based on measurements is not a trivial task. Many recent works have focused on the detection or recognition tasks of environmental sounds [14], [15], [16], [17]. A two-step process is generally followed : describe the audio files with a set of features (Spectral Centroid, harmonicity, Mel-Frequency Cepstral Coefficient ...) and classify them with the help of classifiers (Support Vector Machines, Gaussian Mixture Models, Hidden Markov Model, Artifical Neural Networks). A description of these features and classifiers can be found in [18] and their applications can be found in [19], [20], [21].

The main issue in the detection or recognition tasks is the overlap of environmental sounds. Although near major roads, traffic is predominant, there are many places where it overlaps with other sound sources which contribute significantly to the overall sound levels. To circumvent this issue, Socoró et al. propose to suppress time frames where there is significant overlap by considering an Anomalous Noise Events Detector [22]. It consists in detecting the unwanted sound sources from labeled recordings, *i.e.* that are not related to the traffic component. Those time frames are then discarded in order not to take them into account during the estimation of the traffic sound level. An alternative approach that we will follow in this paper is to consider the blind source separation paradigm to reliably estimate the traffic noise level, see Figure 1. It consists in separating the contribution of the traffic from the other sources within a polyphonic scene. One major advantage of following such approach is that the estimate is continuously available, making the approach applicable in a wide range of urban areas, even where the traffic noise is relatively low compared to the remaining contributions.

In an urban environment context, source separation can be achieved with the help of acoustic microphone arrays and beamforming [23]. However, this approach requires spreading multiple microphones arrays in cities that is very expensive (even with low cost microphones) and time-consuming for calibration and maintenance. This method is then not considered here to be deployed all over cities. In the opposite, monophonic sensor networks need less microphones but the main challenge is to succeed to estimate correctly the road traffic from only one signal in which all kind of sound sources can be present. A convenient method for this is the Non-negative Matrix Factorization (NMF) technique [24]. When considering audio as input, it usually consists in approximating the magnitude spectrogram of an audio file by the product of two low rank matrices, one representing the components of interest and the other the contribution at a given time of those components to approximate the input magnitude spectrogram [25] [26] [27]. In the audio processing domain, NMF has already been employed for the source separation task of monaural signals of speech and music [28] [26]. By design, this method deals reasonably well with the overlapping sound sources as soon as the overlap can be resolved on the time/frequency plane. Closer to our application scenario, NMF has been considered by Innami and Kasai [29]. After having performed NMF on simulated audio files, they perform a source separation in two steps by 1) separating the sound background from the events and 2) by isolating the events using spectral features using a k-means procedure. We study in this paper different flavors of Non-Negative Matrix Factorization where the traffic component is considered in its entirely whether it is a sound background or an event. We demonstrate that supervised NMF and semi supervised NMF approaches have some interests but fail to give satisfactory results for the application at hand. We thus introduce another NMF scheme called thresholded initialized NMF that makes good use of prior knowledge about the source of interest, in our case the traffic noise, but also generalizes well to several kinds of urban areas and to traffic to interference ratio (TIR).

To perform the numerical experiments, we consider a corpus of simulated sound scenes created from a built-up sound database composed of a high number of diverse sound samples. The use of simulated sound scenes is mandatory for rigorous experimental validation as it offers a high level of control on the design of the scenes and the knowledge of the exact contribution of the traffic component ($L_{p,traffic}$), which would be difficult to extract from a recording of an urban scene.

The remaining of the paper is organized as follows. Section 2 details the technical aspects of NMF and describes the 3 approaches considered in this paper to achieve the task at hand. Section 3 describes the corpus of environmental sound scenes and the experimental protocol setup. Section 4 presents and discusses the outcomes of the numerical results.

2 Non-negative Matrix Factorization

2.1 Description of NMF

Non-negative Matrix Factorization is a linear approximation method introduced by Lee and Seung, [24], which can be used to approximate the spectrogram $\tilde{\mathbf{V}}$ (obtained using a Short-Term Fourier Transform) of an audio file,

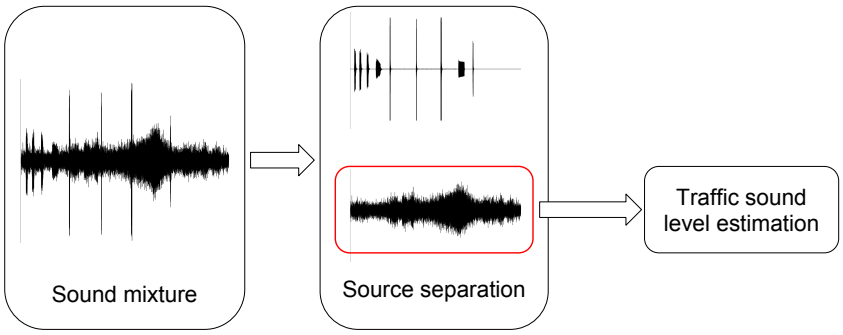

Figure 1: Block diagram of the general source separation model

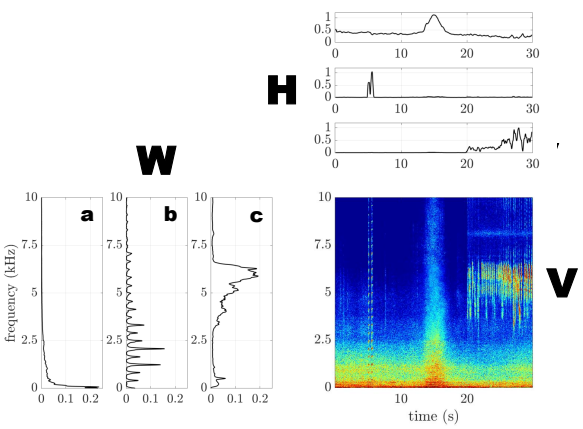

Figure 2: Example of a simple NMF for urban sound mixture composed of 3 sound events (car passages, car horn and bird's whistles), $\mathbf{W}$ is composed of 3 elements too ($K = 3$) which correspond in 3 audio spectra (car passages (a), car horn (b) and bird's whistles (c))

$\mathbf{V}, \in \mathbb{R}^{+}_{F\times N}$ as :

$$\mathbf{V} \approx \tilde{\mathbf{V}} = \mathbf{WH} \tag{1}$$

where $\mathbf{W} \in \mathbb{R}^{+}_{F\times K}$ is the *dictionary* (or basis) matrix composed of audio spectra and $\mathbf{H} \in \mathbb{R}^{+}_{K\times N}$ is the *activation* matrix which summarizes the temporal evolution of each element of $\mathbf{W}$. As the constraint of non-negativity of $\mathbf{W}$ and $\mathbf{H}$ is considered, NMF allows only additive combinations between the element of $\mathbf{W}$. It is then a part-based representation that NMF provides. An illustrative example can be found in Figure 2.

The choice of the dimensions is often made so that $F \times K + K \times N < F \times N$. NMF is then considered as a low rank approximation method. However, this constraint is not mandatory. To estimate the quality of the approximation, an objective function is used

$$\min_{\mathbf{H}\geq 0, \mathbf{W}\geq 0} D\left(\mathbf{V}||\tilde{\mathbf{V}}\right). \tag{2}$$

The operator $D(x|y)$ is a divergence calculation such as:

$$D\left(\mathbf{V}||\tilde{\mathbf{V}}\right) = \sum_{f=1}^{F}\sum_{n=1}^{N} d_\beta\left(\mathbf{V}_{fn}|\left[\mathbf{WH}\right]_{fn}\right) \tag{3}$$

and usually belongs to the $\beta-$divergence class [30] in which the well known Euclidean distance (eq. 4a) and the Kullback-Leibler divergence (eq. 4b) belong

$$d_\beta(x|y) = \begin{cases} \frac{1}{2}(x-y)^2, & \beta = 2, \quad (4a) \\ x\log\frac{x}{y} - x + y, & \beta = 1. \quad (4b) \end{cases}$$

To better take into account prior knowledge about the sources of interest, constraints (like the smoothness or the sparsness criteria [31]) can be added to the objective function.

Algorithms have been proposed to solve the minimization problem (2) iteratively such as the multiplicative update [32], the alternating least square method [33] or the projected gradient [34]. Here, the multiplicative update is chosen as it has been well studied in the literature and it ensures convergence of the results [35].

2.2 Supervised NMF

First, supervised NMF (Sup-NMF) is used: the *dictionary* includes audio spectra of urban sound sources. A lot of the different sound sources present in the urban environment are known. Their spectra can be obtained and be a basis of $\mathbf{W}$. The *activation* matrix is then the unknown variable to estimate. In the first iteration, $\mathbf{H}$ is initialized randomly, then it is updated by the generic algorithm [35]

$$\mathbf{H}^{(i+1)} \leftarrow \mathbf{H}^{(i)}.\left(\frac{\mathbf{W}^T\left[\left(\mathbf{WH}^{(i)}\right)^{(\beta-2)}.\mathbf{V}\right]}{\mathbf{W}^T\left[\mathbf{WH}^{(i)}\right]^{(\beta-1)}}\right)^{\gamma(\beta)} \tag{5}$$

with $\gamma(\beta) = \frac{1}{2-\beta}$, for $\beta < 1$, $\gamma(\beta) = 1$, for $\beta \in [1,2]$ and $\gamma(\beta) = \frac{1}{\beta-1}$ for $\beta > 2$. The product $A.B$ and A/B are respectively the Hadamard product and ratio. As in the supervised approach the indexes of traffic components in $\mathbf{W}$ are known, the separation of the corresponding sound source is made by extracting the related basis and activators,

$$\tilde{\mathbf{V}}_{traffic} = [\mathbf{WH}]_{traffic}\,. \tag{6}$$

2.3 Semi-supervised NMF

The supervised approach is useful when prior knowldge can be assumed for all the sources in the mixture, which is not a reasonable assumption in our application scenario. To some extend, prior knowledge can be considered for the traffic but not for the numerous kind of interferences that can occur in a realistic scenario. To better take into account the diverse nature of urban scenes, semi-supervised NMF (Sem-NMF)[36] is a good candidate as it offers more flexibility. This method assumes a *dictionary* with a fixed part $\mathbf{W_s} \in \mathbb{R}^{+}_{F\times K}$, composed in our case of road traffic spectra, and with a mobile part, $\mathbf{W_r} \in \mathbb{R}^{+}_{F\times J}$ with $J << K$, that is updated during optimization. In the literature, J is set to a small number with respect to K so as to force the optimization to still consider the fixed part of the dictionary [37]. The aim is to include in $\mathbf{W_r}$ the elements that are not related with the traffic. The problem (1) becomes

$$\mathbf{V} \approx \tilde{\mathbf{V}} = \mathbf{W_s H_s} + \mathbf{W_r H_r} \tag{7}$$

with $\mathbf{W} = [\mathbf{W_s W_r}]$ and $\mathbf{H} = \begin{bmatrix}\mathbf{H_s}\\ \mathbf{H_r}\end{bmatrix}$. In a similar way as to solve the equation (2), $\mathbf{W_r}$, $\mathbf{H_r}$ and $\mathbf{H_s}$ are successively updated with the relations (8):

$$\mathbf{W_r}^{(i+1)} \leftarrow \mathbf{W_r}^{(i)} . \left(\frac{\left[\left(\mathbf{W_r H_r}^{(i)}\right)^{(\beta-2)} . \mathbf{V} \right] \mathbf{H_r}^T}{\left(\mathbf{W_r H_r}^{(i)}\right)^{(\beta-1)} \mathbf{H_r}^T} \right)^{\gamma(\beta)}, \tag{8a}$$

$$\mathbf{H_r}^{(i+1)} \leftarrow \mathbf{H_r}^{(i)} . \left(\frac{\mathbf{W_r}^T \left[\left(\mathbf{W_r H_r}^{(i)}\right)^{(\beta-2)} . \mathbf{V} \right]}{\mathbf{W_r}^T \left(\mathbf{W_r H_r}^{(i)}\right)^{(\beta-1)}} \right)^{\gamma(\beta)}, \tag{8b}$$

$$\mathbf{H_s}^{(i+1)} \leftarrow \mathbf{H_s}^{(i)} . \left(\frac{\mathbf{W_s}^T \left[\left(\mathbf{W_s H_s}^{(i)}\right)^{(\beta-2)} . \mathbf{V} \right]}{\mathbf{W_s}^T \left(\mathbf{W_s H_s}^{(i)}\right)^{(\beta-1)}} \right)^{\gamma(\beta)}. \tag{8c}$$

Applications of Sem-NMF for speech denoising from background noise or musical content can be found in [38] and [39].

2.4 Thresholded initialized NMF

As it will be demonstrated in the experimental results described in Section 4, those last approaches fail to provide consistent results in a wide range of urban areas and for different traffic preponderances due to generalization capabilities issues.

We therefore propose an alternative scheme based on the unsupervised NMF. Usually in unsupervised, $\mathbf{W}$, as $\mathbf{H}$, is initialized randomly. Here, as the concerned sound source is known and audio samples of car passages are available, an initial dictionary, $\mathbf{W_0}$, is learnt by converting the audio files in the spectra domain; see part 3.2.1. Then NMF is performed where $\mathbf{W}$ (eq. 9) and $\mathbf{H}$ (eq. 5) are updated alternatively. $\mathbf{W}$ is therefore updated by forcing its initiation with *a priori* knowledge but allowing it to adapt to the actual content of the scene under study,

$$\mathbf{W}^{(i+1)} \leftarrow \mathbf{W}^{(i)} . \left(\frac{\left[\left(\mathbf{W}^{(i)}\mathbf{H}\right)^{(\beta-2)} . \mathbf{V} \right] \mathbf{H}^T}{\left[\mathbf{W}^{(i)}\mathbf{H}\right]^{(\beta-1)} \mathbf{H}^T} \right)^{\gamma(\beta)}. \tag{9}$$

After N iterations, a measure of similarity $D_\theta\left(\mathbf{W_0}||\mathbf{W}\right)$ between $\mathbf{W_0}$ and the obtained dictionary $\mathbf{W}$ for each element k is computed using a cosine similarity metric,

$$D_\theta\left(\mathbf{W_0}_k||\mathbf{W}_k\right) = \frac{\mathbf{W_0}_k . \mathbf{W}_k}{||\mathbf{W_0}_k||.||\mathbf{W}_k||}. \tag{10}$$

$D_\theta\left(\mathbf{W_0}_k||\mathbf{W}_k\right) = 1$ means that the k-th element of $\mathbf{W}$ is identical to the k-th element of $\mathbf{W_0}$. In the opposite, $D_\theta\left(\mathbf{W_0}_k||\mathbf{W}_k\right) = 0$ means that the elements are completely different. This measure is bounded between 1 and 0 and is an invariant with respect to scale. The k value of $D_\theta\left(\mathbf{W_0}||\mathbf{W}\right)$ are next sorted in descending order. The elements in $\mathbf{W}$ that can belong to $\mathbf{W}_{traffic}$ are selected by a *hard thresholding* method. It is defined as:

$$\mathbf{W}_k \in \mathbf{W}_{k,traffic} \quad \text{iff} \quad D\left(\mathbf{W_0}_k||\mathbf{W}_k\right) > t. \tag{11}$$

An illustrative example is displayed in Figure 3.

This approach is named *Thresholded inititialized NMF* (TI-NMF). Other thresholding methods as the *soft* [40] and the *firm* [41] have been investigated. A fast parametric study revealed that the *hard* thresholding method, as presented in Figure 3, was the most reliable approach.

3 Experimental protocol

In order to validate the usefulness of the proposed NMF scheme to estimate the road traffic noise levels, one need

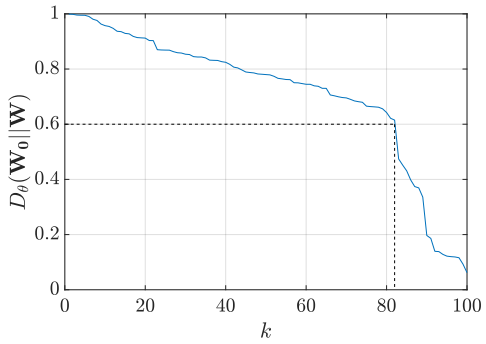

Figure 3: Example of the $\mathbf{W}_{traffic}$ extraction from the sorted cosine similarity with a threshold $t = 0.6$. The 82-nd first elements are considered as traffic component.

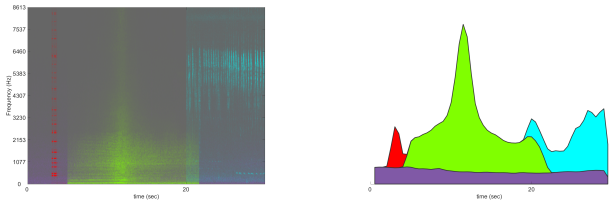

(a) (b)

Figure 4: Example of a simple scene created with *SimScene* software (the spectrogram (a), the time domain b)) with a sound background (road traffic in purple) and 3 sound events (car horn in red, car passage in green and whistling bird in blue)

to compare the traffic noise level predicted by the algorithm to a reference level. The latter can hardly be measured or even annotated from real life recordings. Thus, we propose to consider simulated sound scenes to assess the performance of the proposed NMF. This offers a controlled framework to design at low cost a wide diversity of sound environments in which all the traffic components are known, thus allowing the computation of the reference level.

3.1 Environmental sound scene corpus

The corpus is designed with the *SimScene* software[2]. *SimScene* [42] is a simulator that creates monaural sound scenes in a .wav format by sequencing and summing audio samples that come from an isolated sound database. The simulator has been succesfully considered for a wide range of experimental design for sound detection algorithm assessment [43] [44] [45].

This database is divided into two categories: *i*) the *event* category, which are the brief sounds (from 1 to 20 seconds) that are considered as salient including 245 sound event samples divided in 19 sound classes (*ringing bell, whistling bird, sweeping broom, car horn, passing car, hammer, drill, coughing, barking dog, rolling suitcase, closing door, plane, siren, footstep, storm, street noise, metallic noise, train, tramway, truck and voice*) and *ii*) the *background* or *texture* category that includes all the sounds that are of long duration and whose acoustic properties do not vary with respect to time. 154 sound samples that belong to this category are divided in 9 sound classes (*whistling bird, construction site noise, crowd noise, park, rain, children playing in schoolyard, constant traffic noise, ventilation, wind*). These sounds are in .wav format sampled at 44.1 kHz. The sound class *car passages* comes from 60 recordings of 2 cars (Renault Megane and Renault Scenic) made on the Ifsttar's runway at different speeds with multiple gear ratio. The other audio files have been found online (*freesound.org*) and within the *UrbanSound8k* database [46]. Each sound class is composed of multiples samples (*bird01.wav*, *bird02.wav* ...) to allow some diversity in the resulting mixture, see Figure 4. The software allows the user to control some high level parameters (number of events of each class that appear in the mixture, elapsed time between each sample of a same class, presence of a fade in and a fade out ...) completed with a standard deviation that may bring some random behavior between the scenes. Furthermore, an audio file of each sound class present in the scene can be generated that allows to know its exact contribution as well as a text file that summarizes the time presence of all the events.

This database allows us to create a wide diversity of realistic urban sound scenes from the road traffic point of view [47]. A sound mixing corpus is composed of 6 sub-corpus of 25 audio files each lasting 30 seconds. Each sub-corpus is characterized by a specific generic sound class that summed with traffic will make the estimation of the traffic level more difficult. The classes are: *alert* (car horn, siren), *animals* (barking dog , whistling bird), *climate* (wind, rain), *humans* (crowd noise and voice), *mechanics* (metallic and construction site noises) and *transportation* (train, tramway and plane). In each file, traffic component is present as the sum of the background and event traffic sounds while the *interfering* sound class is the sound sources not related to it. To test different scenarios, each audio file is duplicated with the traffic sound level of the entire sound scene, $L_{p,traffic}$, fixed to a specific level according to the sound level of the interfering class, $L_{p,interfering}$, following the relation (12).

$$TIR = L_{p,traffic} - L_{p,interfering} \tag{12}$$

[2]Open-source project available at: https://bitbucket.org/mlagrange/simScene

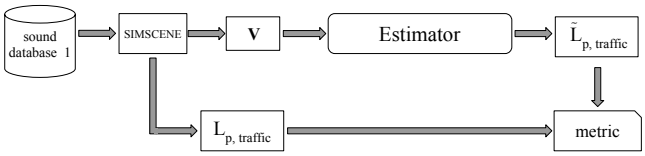

Figure 5: Block diagram of the experience with the urban sound scenes sound mixture step and the estimation step. The estimator may be a frequency low-pass filter or NMF

with the *Traffic Interference Ratio* $TIR \in$ [-12 -6 0 6 12] dB. When $TIR < 0$ dB, the traffic component is less present than the interfering class. In the opposite, for $TIR > 0$ dB, the traffic class is louder than the interfering class. The total number of scenes designed is 750 (6 sub-corpus $\times$ 25 scenes $\times$ 5 TIR values). The corpora are available for download at: https://zenodo.org/record/1145855#.Wl2oPnkiGos

3.2 Experiment

The experiment consists in estimating the road traffic sound level of the 6 environmental sound sub-corpus (*alert* (al), *animals* (an), *humans* (hu), *climate* (cl), *mechanics* (me), *transportation* (tr)) composed each of 25 audio files ($M = 25$) and for 5 TIR ([-12 -6 0 6 12] dB). The spectrogram $\mathbf{V}$ of each sound scene is built with a window size $w = 2^{12}$ with a 50 % overlap, see Figure 5.

Assuming that the traffic spectral profile is largely concentrated in the low frequency components, a first estimator to determine the traffic sound level is a frequency low-pass filter. It depends only on the cut-off frequencies $f_c \in$ [500 1k 2k 5k 10k 20k] Hz. The spectrogram $\mathbf{V}$ is filtered and the remaining energy is then considered as traffic component (eq. 13),

$$\tilde{\mathbf{V}}_{traffic} = \mathbf{V}_{f_c}. \tag{13}$$

The second estimator is the proposed scheme, based on the three NMF schemes presented in Section 2. Multiples experimental factors are involved here between the dictionary learning and NMF (see Figure 6), each experimental factor having multiples modalities.

3.2.1 NMF Dictionary

In order to prevent potential overfitting issues, the dictionary is built from a separate sound database dedicated specifically to this task. It is composed of 53 audio files of passing cars. These recordings have been made on the Ifsttar's runway too, with the same experimental conditions that the recordings of the *SimScene* database but with two different cars (Dacia Sandero and Renault Clio). First, for each audio file, its spectrogram is calculated with fixed parameters (w, 50 % overlap, $nfft$). Then time/frequency windows of $F \times w_t$ dimensions are applied without overlapping on the spectrogram in order to consider several spectra for each audio file where $w_t \in$ [0.5 1] second. In each window, the root mean square value is calculated on each frequency bin to reduce the windowed spectrogram in one spectrum a of $F \times 1$ dimension. With this size of window, it is possible to obtain the characteristic pitches of the different audio samples. One obtain for each value of w_t, from the 53 audio samples of passing cars respectively 2218 and 1109 elements. Since the number of elements given by this processing is high, in order to reduce the computational time and avoid redundant information, a K-means clustering algorithm is applied to reduce the number of spectra to $K \in$ [25, 50, 100, 200]. The K centroids are then the elements considered in the dictionary. A special case is added where the root mean square of *all* the spectrogram is applied ($w_t = all$) in order to build a dictionary with the spectral envelope of each audio sample. In this case, 53 spectra are obtained. The K-means clustering algorithm is then reduced to $K \in$ [25 50].

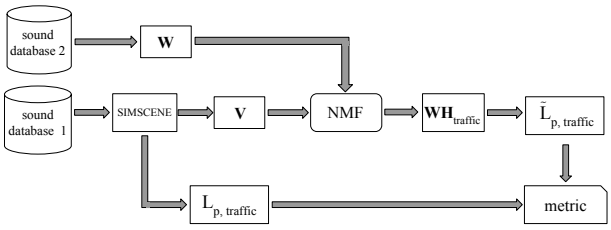

Figure 6: Specific block diagram of the NMF estimator with the dictionary design composed from a second sound database

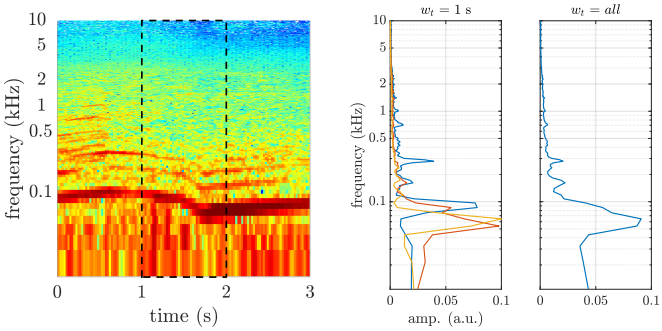

(a) (b)

Figure 7: Example of the dictionary building with a 3 second extract of a car passage. In dashed lines, a 1 second w_t window (a). With $w_t = 1$ second, 3 spectra are then generated and included in $\mathbf{W}$, while for $w_t = all$, the audio file is reduced into 1 spectral vector (b)

experimental factors	**modalities**						**number of modality**
sub-classes	alert	animals	climate	humans	transportation	mechanics	6
TIR (dB)	-12	-6	0	6	12		5
$\mathbf{f_c}$ (kHz)	0.5	1	2	5	10	20	6

Table 1: Summary of the different experimental factors and their modalities taken into account in the frequency low-pass filter estimator

experimental factors	**modalities**						**number of modality**
sub-classes	alert	animals	climate	humans	transportation	mechanics	6
TIR (dB)	-12	-6	0	6	12		5
method	Sup-NMF		Sem-NMF		TI-NMF		3
$\mathbf{w_t}$ (s)	0.5		1		*all*		3
K	25	50	100		200		4
β	1			2			2
t	from 0.30 to 0.70 with 0.01 step						40

Table 2: Summary of the different experimental factors and their modalities taken into account in NMF estimator

An example that illustrates the process can be found on Figure 7 on a 3 second extract of the spectrogram of a car passage, see Figure 7a. In the case where w_t = 1 second, 3 elements are therefore extracted from the spectrogram while in the case where $w_t = all$, all the spectrogram is reduced into one element, see Figure 7b.

The obtained dictionary is expressed with third octave bands and each basis vector of $\mathbf{W}$ is normalized such as $||\mathbf{W_k}|| = 1$ with $||\bullet||$ the ℓ-1 norm. Table 2 summarizes the experimental factors (K and w_t) for the dictionary building and their related modalities. This last step allows us to reduce the dimensionality while preserving a rich description of the spectral content. Experimental validation consistently showed that considering octave bands do not impact the performance of the estimator studied in this paper.

3.2.2 Experimental factors of NMF

Sup-NMF and Sem-NMF updates are computed for 400 iterations, which is sufficient to reach convergence. TI-NMF is performed on a lower number of iterations (60) to prevent $\mathbf{W}$ to not deviate too much from the initial dictionary. The spectrogram $\mathbf{V}$ and the dictionary $\mathbf{W}$ are expressed with third octave bands (F = 29). This coarser method allows the reduction of the matrix size and decreases the computation time. But, must of all, by expressing the frequency axis on a log frequency axis, the low frequencies, where the traffic energy is focused, are described more finely than the high frequencies. For TI-NMF, the threshold t is set between 0.30 and 0.70 with a step of 0.01. Tables 1 and 2 summarize the experimental factors and their related modalities.

Considering the experimental settings derived from the different modalities of each experimental factor described in Table 1 between the 5 levels of TIR, the 6 sub-classes and the 6 cut-off frequencies f_c, 180 settings are performed. For Sup-NMF and Sem-NMF, according to Table 2, 1200 associations of factors are made where the 4 levels of K are associated with $w_t \in$ [0.5 1] s whereas only 2 levels of K (25 and 50) are associated with $w_t = all$, see part 3.2.1. For TI-NMF, 24000 combinations are computed. In all, 25380 settings are performed between the different forms of the dictionary $\mathbf{W}$ and the multiple experimental factors.

For each setting, the estimator (frequency low-pass filter or NMF) is performed on the M scenes of a sub-class. For one sound scene, the average traffic sound level, $\tilde{L}_{p,traffic}$, of the entire scene is calculated,

$$\tilde{L}_{p,traffic} = 20\log_{10}\left(\frac{p_{rms}}{p_0}\right) \tag{14}$$

where p_{rms} is the effective pressure deducted from the remaining spectrogram ($\mathbf{V}_{f_c}$ or $[\mathbf{WH}]_{traffic}$) and p_0 is the reference sound pressure, $p_0 = 2\times10^{-5}Pa$. For each setting of experimental factors, M values of $\tilde{L}_{p,traffic}$, corresponding to the M scenes, are then obtained and are compared to the M exact sound level, $L_{p,traffic}$.

method	f_c (kHz)	β	**K**	$\mathbf{w_t}$ (s)	**t**	MAE (dB)
filter	20					4.69 ($\pm$ 4.52)
filter	0.5					2.89 ($\pm$ 2.84)
Sup-NMF		1	50	0.5		3.44 ($\pm$ 3.70)
Sup-NMF		2	50	0.5		3.02 ($\pm$ 3.33)
Sem-NMF		1	100	0.5		2.33 ($\pm$ 1.10)
Sem-NMF		2	100	0.5		2.32 ($\pm$ 1.26)
TI-NMF		**1**	**200**	**0.5**	**0.42**	**2.19 ($\pm$ 2.18)**
TI-NMF		2	25	all	0.54	2.20 ($\pm$ 2.26)

Table 3: Best results for all the scenes according to the experimental factors β and *method* (in bold letter, the lowest error).

method	filter	filter	Sup-NMF	Sem-NMF	TI-NMF
f_c (kHz)	20	0.5			
β			2	2	1
-12	12.25 ($\pm$ 0.05)	7.36 ($\pm$ 3.00)	8.65 ($\pm$ 1.88)	3.88 ($\pm$ 1.52)	5.35 ($\pm$ 2.71)
-6	6.96 ($\pm$ 0.05)	3.44 ($\pm$ 1.65)	4.22 ($\pm$ 1.27)	1.37 ($\pm$ 0.71)	2.82 ($\pm$ 1.30)
0	3.00 ($\pm$ 0.03)	1.17 ($\pm$ 0.24)	1.34 ($\pm$ 0.56)	1.11 ($\pm$ 0.25)	1.26 ($\pm$ 0.35)
6	0.25 ($\pm$ 0.06)	1.03 ($\pm$ 0.26)	0.26 ($\pm$ 0.10)	2.25 ($\pm$ 0.19)	0.70 ($\pm$ 0.32)
12	0.26 ($\pm$ 0.00)	1.45 ($\pm$ 0.13)	0.64 ($\pm$ 0.06)	2.96 ($\pm$ 0.21)	0.84 ($\pm$ 0.24)

Table 4: MAE error averaged on all sub-classes on each TIR for the best scenario according to each method

3.2.3 Metrics

The performance of the road traffic sound level estimator is assessed through the calculation of one reference metric, the Mean Absolute Error (MAE) [48]. It expresses the quality of the long-term reconstruction of the signal and consists in the average over the M sound scenes of the absolute difference between the exact and estimated traffic sound level in dB,

$$MAE = \frac{\sum_{m=1}^{M} |L^m_{p,traffic} - \tilde{L}^m_{p,traffic}|}{M}. \qquad (15)$$

4 Results

Table 3 summarizes, according to the 2 main factors (*method*, β), the lowest MAE error averaged on all sub-classes and all TIR (750 sound mixtures in all). For the low-pass frequency filters and each NMF approaches, the best parameter combinations are detailed according to the TIR in Table 4, and are expanded to the sub-classes in Figures 9a, 9b, 9c and 9d.

First, the errors produced by the filter are detailed. f_c = 20 kHz is equivalent to consider all the sound mixtures without distinction between traffic and others sound sources. Consequently, in low TIR (-12 dB and -6 dB), where traffic component is scarce, the error is more important than in high TIR (6 dB and 12 dB) where the traffic component is predominant. f_c = 500 Hz is the cut-off frequency with the lowest mean error obtained. It is then considered as the baseline to compare the performances of NMF.

In low TIR, for *alert* and *animals*, which are sub-classes composed of higher frequencies, this filter is efficient as it removes these frequency components. For the other sub-classes where low frequency contents are present (storm for *climate*, voices in *humans*, planes, tramway and train in *transport* and ventilation noise in *mechanics*), the filter considers all the energy located in the pass-band and then does not dissociate the traffic element from the other sound sources. The errors are then nearly all superior to 4 dB and are overestimated, see Figure 8a. In opposite, in high TIR, the error is due to the energy removed from the traffic which has the consequence to underestimate the sound levels, see Figure 8b. The 500 Hz filter finds a balance between what is put aside in low TIR and what it is remained in high TIR.

Compared with the filter errors, the choice of some NMF approaches makes it possible to decrease the error of the road traffic sound level estimation. The supervised approach is the only method that has an average error superior to the 500 Hz filter baseline. Sem-NMF and

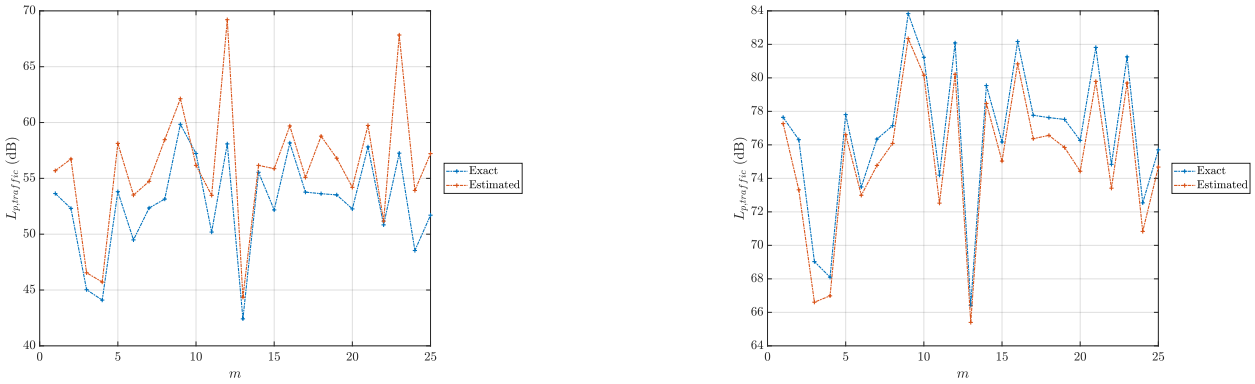

(a) (b)

Figure 8: Global sound levels of the traffic estimated by the frequency low-pass filter with $f_c = 500$ Hz for the M scenes of the sub-classes *alert* at $TIR = -12$ dB(a) and at $TIR = 12$ dB (b)

TI-NMF have better results. The lowest average error is obtained for TI-NMF, 2.19 ± 2.18, for $\beta = 1$ and threshold $t = 0.42$ with the dictionary factors $K = 200$ and $w_t = 500$ ms. On the other hand, the semi-supervised approach has a higher error but a lower standard deviation (2.32 ± 1.26).

According to Table 4 and Figures 9, the behavior between the 3 versions of NMF differs. In the case of Sup-NMF, it fails to improve the filtering performances despite good results in high TIR. The errors are too important for low TIR and this for all the sub-classes. This method reveals to be too rigid as $\mathbf{W}$ is composed of fixed traffic spectra. In the case of low TIR, in the aim to reduce the objective function, see eq. 2, traffic elements are used whatever the sound event in the sound scene. In order to expose this issue, the case of a scene of the *alert* sub-class is presented in Figure 10a. Here when the *alert* sub-class sounds, some traffic elements of $\mathbf{W}$ are activated. The *alert* sub-class is then considered as traffic component generating a wrong estimation of the sound level, see Figure 10a. This behavior disappears when the traffic component becomes predominant to the interfering class as in Figure 10b. Thus forcing the dictionary to be only traffic spectra is not a sufficient way to estimate correctly the traffic sound level, $\tilde{L}_{p,traffic}$.

Consequently, with the addition of a mobile part in the dictionary, $\mathbf{W_r}$, the semi-supervised approach allows a better consideration of the interfering class in low TIR. It brings a significant decrease of the errors for low TIR as it can be seen in Figure 9c. The content of $\mathbf{W_r}$, in the case of an *alert* sub-class is displayed in Figure 11a. The interfering class is easily integrated. The first element is mainly composed of high frequency bands which correspond to the car horns of the scene. This composition impacted directly the traffic sound level estimation as it can be seen in Figure 10a where the elements of the dictionary dedicated to the traffic are no longer activated when the car horn is active.

However, the relatively high degrees of freedom of Sem-NMF are restrictive for high TIR as the errors exceed 2 dB for all sub-classes and increase with $TIR =$ 6 dB and 12 dB. In order to reduce $D(\mathbf{V}||\mathbf{WH})$, without constraint, Sem-NMF is free to include traffic components in $\mathbf{W_r}$. Consequently, this behavior decreases the quality of the reconstruction of the traffic component. In Figure 11b for $TIR = 12$ dB, the high frequency components of the alert sounds are lower for the benefit of low frequency content. Consequently, the traffic sound level estimation is then underestimated as in Figure 10b.

Finally, TI-NMF with a threshold $t = 0.42$ and $\beta = 1$, offers the lowest average error (Table 3). Unlike Sup-NMF, where $\mathbf{W}$ is fixed, and Sem-NMF, where only $\mathbf{W_r}$ is updated, TI-NMF updates $\mathbf{W}$ entirely to adjust prior knowledge to the scene under evaluation so as to adapt to the different sound environments. The closest elements of the traffic component defined in $\mathbf{W_0}$ are then extracted to deduce the traffic signal. In Figure 12, the similarity $D_\theta(\mathbf{W_0}||\mathbf{W})$ is displayed for 3 sub-classes and $TIR \in$ [-12, 12] dB.

For low TIR, as the traffic sound class is not predominant, the final dictionary strongly differs from the $\mathbf{W_0}$. With the thresholding, only a reduced number of basis vectors are considered as traffic components. In comparison to supervised results, this approach reduces significantly the error for the *human* and *transport* sub-classes. However, for *climate* and *mechanics*, the errors remain important as these interfering classes have similar spectral profiles when compared to traffic ones.

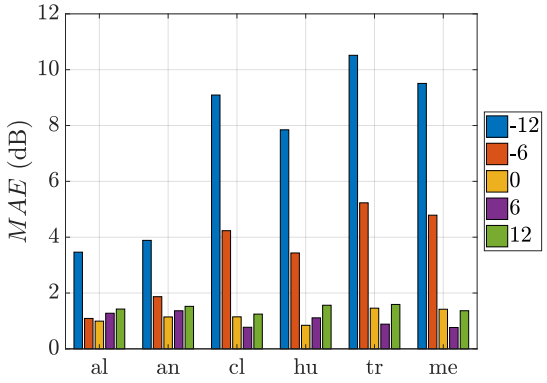

(a) Frequency low-pass filter with $f_c = 500$ Hz

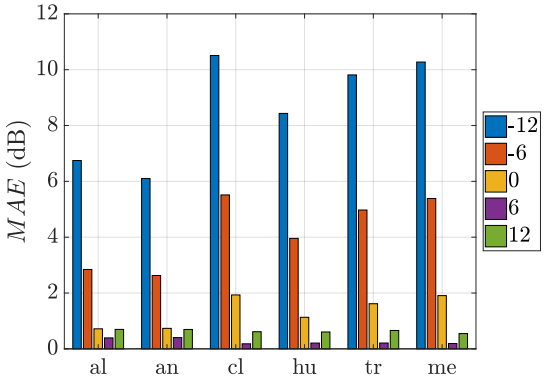

(b) MAE error for each TIR and sub-class with Sup-NMF and $\beta = 2$

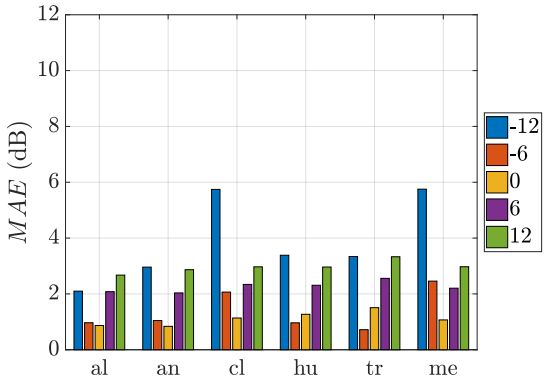

(c) MAE error for each TIR and sub-class with Sem-NMF and $\beta = 2$

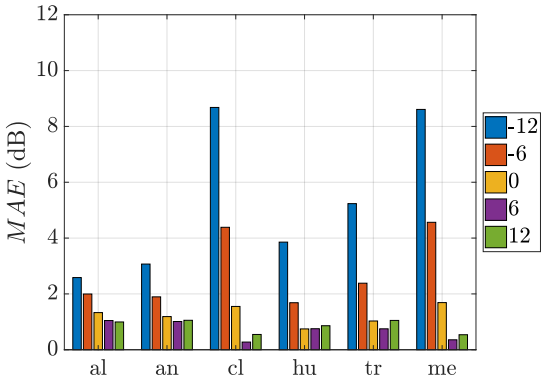

(d) MAE error for each TIR and sub-class with TI-NMF, $\beta = 1$ and $t = 0.42$

Figure 9: MAE error for each sub-class and each TIR according to the the best results with the filter (a) and each method (Sup-NMF (b), Sem-NMF (c) and TI-NMF (d))

For high TIR, as the traffic is the main sound source, the similarity of the initial dictionary and $\mathbf{W}$ is higher which allows retaining more elements as traffic components and then decreases the error (< 1 dB). The kept elements are then more suited to the scenes than a fixed dictionary. The error for these TIR is then due to the thresholding which put aside some elements that are nevertheless related to the traffic component. With a low threshold, it is possible to decrease the error. For TIR = 12 dB, the average error on all the sub-classes is 0.22 ($\pm$ 0.08) dB with $t = 0.30$. In opposite for TIR = -12 dB, it is better to choose a high threshold $t = 0.55$, the error decrease then to 4.46 $\pm$ 1.66. In order to generalize this method where no prior knowledge on the urban environment, the chosen threshold t is then fixed to t = 0.42 and is the one that best balanced these opposite cases.

5 Conclusion

In this work the non negative metric factorization framework was used to estimate the road traffic sound level in urban sound mixtures. It is a well suited approach to these sound environments because it easily takes into account the overlap between the multiple sound sources present in the cities and it is adapted to monophonic sensor networks. Different versions of NMF have been studied as a supervised and semi-supervised approach. On a large corpus of sounds, the supervised approach proves to be too restrictive to be adapted to different sound environments whereas the semi-supervised approach has, on the contrary, too many degrees of freedom on the mobile dictionary $\mathbf{W_r}$, decreasing its performance especially when the traffic is predominant. The proposed approach, named threshold initialized NMF achieves the lowest average error. With this method, the $\mathbf{W}$ is initialized with road traffic spectra, updated and the dictionary elements

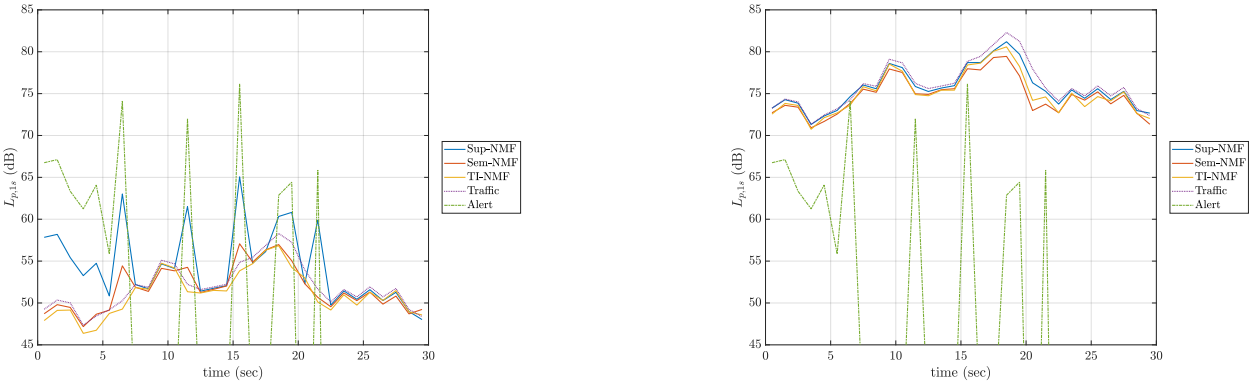

(a) (b)

Figure 10: 1 second equivalent sound pressure level of an *alert* sub-class scene for supervised NMF ($\beta = 2$, $K = 50$, $w_t = 0.5$ s), semi-supervised ($\beta = 2$, $K = 100$, $w_t = 0.5$ s) and thresholded initialized ($\beta = 1$, $K = 200$, $w_t = 0.5$ s, $t = 0.42$) at $TIR = -12$ dB(a) and $TIR = 12$ dB (b)

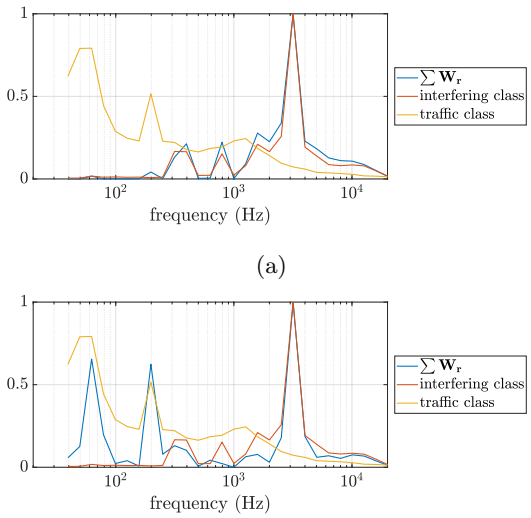

(a)

(b)

Figure 11: Comparison between the sum of the 2 elements of $\mathbf{W_r}$ with the spectra of the interfering and traffic classes for an *alert* scene for TIR = -12 dB (a) and $TIR = 12$ dB (b) with $\beta = 2$, $K = 100$ and $w_t = 0.5$ s (normalized amplitudes)

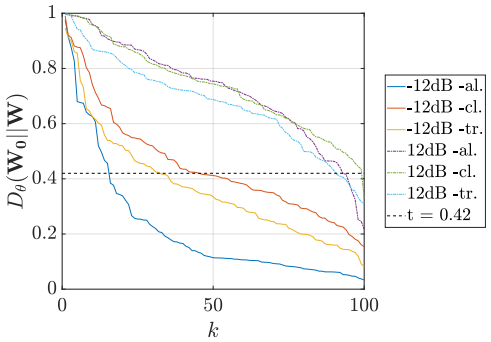

Figure 12: Example of the similarity $D_\theta(\mathbf{W_0}||\mathbf{W})$ for different sub-classes and for two TIR (-12 dB and 12 dB) and with the threshold $t = 0.42$ ($\beta = 1$, $K = 200$ and $w_t = 0.5$ s)

that are similar to the road traffic spectra are then extracted by hard thresholding. A major advantage of the proposed approach is that it is not designed for a specific source. Even though the experiments described in this paper focused on traffic sounds, changing the dictionary to contain bird sounds would lead to an estimator of the presence of birds. Extending the apporach to other sources is thus of intetrest for future research. Also, performance improvement could be achieved by the addition of constraints such as sparsness [49] and smoothness [31] of the low rank matrices.

The experimental protocol and the evaluated estimators have been implemented with the Matlab software. For reproducible purposes, the code is available online[3].

[3] https://github.com/jean-remyGloaguen/article2017EstimationAmbiance

The evaluation database composed of multiple samples of urban sounds is also made available for the research community with interest in detection, separation and recognition tasks of urban sound sources.

References

[1] H. Van Leeuwen and S. Van Banda. Noise mapping - State of the art - Is it just as simple as it looks? *EuroNoise*, 2015.

[2] O. Leroy, B. Gauvreau, F. Junker, E. De Rocquigny, and M. Berengier. Uncertainty assessment for outdoor sound propagation. In *20th International Congress on Acoustics, ICA 2010*, page 7p, France, August 2010.

[3] N. Garg and S. Maji. A Critical Review of Principal Traffic Noise Models: Strategies and Implications. *Environmental Impact Assessment Review*, 46, April 2014.

[4] W. Wei, T. Van Renterghem, B. De Coensel, and D. Botteldooren. Dynamic noise mapping: A map-based interpolation between noise measurements with high temporal resolution. *Applied Acoustics*, Complete(101):127–140, 2016.

[5] P. Mioduszewski, J. A. Ejsmont, J. Grabowski, and D. Karpinski. Noise map validation by continuous noise monitoring. *Applied Acoustics*, 72(8):582–589, july 2011.

[6] C. Mietlicki, F. Mietlicki, and M. Sineau. An innovative approach for long-term environmental noise measurement: Rumeur network. In *INTER-NOISE and NOISE-CON Congress and Conference Proceedings*, volume 2012, pages 7119–7130. Institute of Noise Control Engineering, 2012.

[7] A. Can, T. Van Renterghem, and D. Botteldooren. Exploring the use of mobile sensors for noise and black carbon measurements in an urban environment. In Société Française d'Acoustique, editor, *Acoustics 2012*, Nantes, France, April 2012.

[8] D. Manvell, L. Ballarin Marcos, H. Stapelfeldt, and R. Sanz. Sadmam-combining measurements and calculations to map noise in madrid. In *INTER-NOISE and NOISE-CON Congress and Conference Proceedings*, volume 2004, pages 1998–2005. Institute of Noise Control Engineering, 2004.

[9] S. Xavier, S. J. Claudi, A. Francesc, B. Patrizia, and al. DYNAMAP – Development of low cost sensors networks for real time noise mapping. *Noise Mapping*, 3(1), May 2016.

[10] P. Bellucci, L. Peruzzi, and G. Zambon. LIFE DYNAMAP project: The case study of Rome. *Applied Acoustics*, Part B(117):193–206, 2017.

[11] C. Mydlarz, J. Salamon, and J. P. Bello. The implementation of low-cost urban acoustic monitoring devices. *Applied Acoustics*, 117:207–218, 2017.

[12] Justin Salamon and Juan Pablo Bello. Deep convolutional neural networks and data augmentation for environmental sound classification. *IEEE Signal Processing Letters*, 24(3):279–283, 2017.

[13] J. Picaut, A. Can, J. Ardouin, P. Crépeaux, T. Dhorne, D. Écotière, M. Lagrange, C. Lavandier, V. Mallet, C. Mietlicki, et al. Characterization of urban sound environments using a comprehensive approach combining open data, measurements, and modeling. *The Journal of the Acoustical Society of America*, 141(5):3808–3808, 2017.

[14] T. Heittola, A. Mesaros, T. Virtanen, and A. Eronen. Sound event detection in multisource environments using source separation. In *in Workshop on Machine Listening in Multisource Environments, CHiME2011*, 2011.

[15] B. Defreville, F. Pachet, C. Rosin, and P. Roy. Automatic Recognition of Urban Sound Sources. Audio Engineering Society, 2006.

[16] A. Dufaux, L. Besacier, M. Ansorge, and F. Pellandini. Automatic sound detection and recognition for noisy environment. In *2000 10th European Signal Processing Conference*, pages 1–4, September 2000.

[17] S. Chu, S. Narayanan, and C. C. J. Kuo. Environmental Sound Recognition With Time-Frequency Audio Features. *IEEE Transactions on Audio, Speech, and Language Processing*, 17(6):1142–1158, August 2009.

[18] M. Cowling and R. Sitte. Comparison of techniques for environmental sound recognition. *Pattern Recognition Letters*, 24(15):2895–2907, November 2003.

[19] G. Shen, Q. Nguyen, and J. Choi. An Environmental Sound Source Classification System Based on Mel-Frequency Cepstral Coefficients and Gaussian Mixture Models. *IFAC Proceedings Volumes*, 45(6):1802–1807, May 2012.

[20] F. Beritelli and R. Grasso. A pattern recognition system for environmental sound classification based on MFCCs and neural networks. In *2008 2nd International Conference on Signal Processing and Communication Systems*, pages 1–4, December 2008.

[21] L. Couvreur and M. Laniray. Automatic Noise Recognition in Urban Environments Based on Artificial Neural Networks and Hidden Markov Models. In *The 33 rd International Congress and Exposition on Noise Control Engineering*, Prague, August 2004.

[22] J. C. Socoró, F. Alías, and R. M. Alsina-Pagès. An Anomalous Noise Events Detector for Dynamic Road Traffic Noise Mapping in Real-Life Urban and Suburban Environments. *Sensors*, 17(10):2323, October 2017.

[23] H. Saruwatari, S. Kurita, K. Takeda, F. Itakura, T. Nishikawa, and K. Shikano. Blind source separation combining independent component analysis and beamforming. *EURASIP Journal on Applied Signal Processing*, 2003:1135–1146, 2003.

[24] D. D. Lee and H. S. Seung. Learning the parts of objects by non-negative matrix factorization. *Nature*, 401(6755):788–791, October 1999.

[25] P. Smaragdis and J.C. Brown. Non-negative matrix factorization for polyphonic music transcription. In *Applications of Signal Processing to Audio and Acoustics, 2003 IEEE Workshop on.*, pages 177–180, October 2003.

[26] K. W. Wilson, B. Raj, P. Smaragdis, and A. Divakaran. Speech denoising using nonnegative matrix factorization with priors. In *2008 IEEE International Conference on Acoustics, Speech and Signal Processing*, pages 4029–4032, March 2008.

[27] A. Mesaros, T. Heittola, O. Dikmen, and T. Virtanen. Sound event detection in real life recordings using coupled matrix factorization of spectral representations and class activity annotations. In *2015 IEEE International Conference on Acoustics, Speech and Signal Processing (ICASSP)*, pages 151–155, April 2015.

[28] B. Wang and M. D. Plumbley. Musical audio stream separation by non-negative matrix factorization. *Proc. DMRN summer conf*, pages 23–24, 2005.

[29] I. Satoshi and K. Hiroyuki. NMF-based environmental sound source separation using time-variant gain features. *Computers & Mathematics with Applications*, 64(5):1333–1342, 2012.

[30] C. Févotte, N. Bertin, and J. Durrieu. Nonnegative matrix factorization with the Itakura-Saito divergence: with application to music analysis. *Neural Computation*, 21(3):793–830, March 2009.

[31] T. Virtanen. Monaural Sound Source Separation by Nonnegative Matrix Factorization With Temporal Continuity and Sparseness Criteria. *IEEE Transactions on Audio, Speech, and Language Processing*, 15(3):1066–1074, March 2007.

[32] D. Lee and H. Seung. Algorithms for Non-negative Matrix Factorization. In *In NIPS*, pages 556–562. MIT Press, 2000.

[33] A. Cichocki and R. Zdunek. Regularized Alternating Least Squares Algorithms for Non-negative Matrix/Tensor Factorization. In *Advances in Neural Networks – ISNN 2007*, Lecture Notes in Computer Science, pages 793–802. Springer, Berlin, Heidelberg, June 2007.

[34] C. J. Lin. Projected Gradient Methods for Nonnegative Matrix Factorization. *Neural Computation*, 19(10):2756–2779, October 2007.

[35] C. Févotte and J. Idier. Algorithms for nonnegative matrix factorization with the β-divergence. *Neural Computation*, 23(9):2421–2456, 2011.

[36] H. Lee, J. Yoo, and S. Choi. Semi-Supervised Nonnegative Matrix Factorization. *IEEE Signal Processing Letters*, 17(1):4–7, January 2010.

[37] A. Lefevre, F. Bach, and C. Févotte. Semi-supervised NMF with time-frequency annotations for single-channel source separation. In *ISMIR 2012: 13th International Society for Music Information Retrieval Conference*, 2012.

[38] C. Joder, F. Weninger, F. Eyben, D. Virette, and B. Schuller. Real-time speech separation by semi-supervised nonnegative matrix factorization. *Latent Variable Analysis and Signal Separation*, pages 322–329, 2012.

[39] F. Weninger, J. Feliu, and B. Schuller. Supervised and semi-supervised suppression of background music in monaural speech recordings. In *Acoustics, Speech and Signal Processing (ICASSP), 2012 IEEE International Conference on*, pages 61–64. IEEE, 2012.

[40] D. L. Donoho. De-noising by soft-thresholding. *IEEE transactions on information theory*, 41(3):613–627, 1995.

[41] M. Fornasier and H. Rauhut. Iterative thresholding algorithms. *Applied and Computational Harmonic Analysis*, 25(2):187–208, 2008.

[42] M. Rossignol, G. Lafay, M. Lagrange, and N. Misdariis. SimScene: a web-based acoustic scenes simulator. In *1st Web Audio Conference (WAC)*, 2015.

[43] G. Lafay, M. Lagrange, M. Rossignol, E. Benetos, and A. Roebel. A morphological model for simulating acoustic scenes and its application to sound event detection. *IEEE/ACM Transactions on Audio, Speech and Language Processing*, 24(10):1854–1864, 2016.

[44] E. Benetos, G. Lafay, M. Lagrange, and M. D. Plumbley. Polyphonic Sound Event Tracking using Linear Dynamical Systems. *IEEE Transactions on Audio, Speech and Language Processing*, May 2017.

[45] A. Mesaros, T. Heittola, E. Benetos, P. Foster, M. Lagrange, T. Virtanen, and M. D. Plumbley. Detection and Classification of Acoustic Scenes and Events: Outcome of the DCASE 2016 Challenge. *IEEE/ACM Transactions on Audio, Speech and Language Processing*, 2017.

[46] J. Salamon, C. Jacoby, and J. P. Bello. A dataset and taxonomy for urban sound research. In *22st ACM International Conference on Multimedia (ACM-MM'14)*, Orlando, FL, USA, Nov. 2014.

[47] J.-R. Gloaguen, A. Can, M. Lagrange, and J.-F. Petiot. Creation of a corpus of realistic urban sound scenes with controlled acoustic properties. *The Journal of the Acoustical Society of America*, 141(5):4044–4044, May 2017.

[48] C. J. Willmott and K. Matsuura. Advantages of the mean absolute error (mae) over the root mean square error (rmse) in assessing average model performance. *Climate research*, 30(1):79–82, 2005.

[49] P. O. Hoyer. Non-negative matrix factorization with sparseness constraints. *Journal of machine learning research*, 5(Nov):1457–1469, 2004.